Preprints, 4th IFAC Conference on
Advances in Proportional-Integral-Derivative Control
Almería, Spain | June 12-14, 2024

Cascade motion control with synchronised saturation ⋆

Daniel Bilbao-Moreno * **Iker Elorza** * **Eloy Irigoyen** **

* *IKERLAN, Paseo José María Arizmendiarreta 2, Arrasate/Mondragon, 20500, Spain (e-mail: dbilbao@ikerlan.es; ielorza@ikerlan.es).*
** *Department of Automatic Control and Systems Engineering, Universidad del País Vasco, UPV/EHU, Pl. Ingeniero Torres Quevedo, Bilbao, 48013, Spain (e-mail: eloy.irigoyen@ehu.eus)*

Abstract: This paper introduces an innovative motion control scheme tailored for traction systems, employing a cascade PI controller architecture. The internal loop regulates speed, and the external loop generates the necessary speed setpoint for position control. Two feedforward actions are strategically implemented in each loop to address potential disturbances and optimise overall performance. An inherent challenge in cascade control systems is the phenomenon known as windup, where integral components accumulate errors due to persistent disturbances or sudden changes in position reference. In order to mitigate this phenomenon, a control approach which integrates corresponding saturations for each loop and ensures synchronisation between them is developed. In this way, the external loop does not generate speed setpoints beyond physical thresholds during internal loop saturation. This strategic limitation prevents overly aggressive responses and eliminates undesired traction demands during saturation events. The proposed control scheme is validated through simulations that incorporate various disturbances, and the analysis of results confirms its suitability, showcasing improvements in the performance of such control schemes, especially in scenarios prone to windup.

Keywords: Cascade control, motion control, windup, saturation, synchronisation, PID control, feedforward actions.

1. INTRODUCTION

Speed control has been a predominant approach in the realm of high-level control for traction systems, going back to the early days of James Watt's centrifugal governor, among others (Maxwell, 1868). Modern applications of this principle can be seen, for example, in cruise control for electric vehicles, where only PID-based speed controllers were initially employed (Shakouri et al., 2011; Dantas et al., 2018). However, the evolution of targets in terms of position, not just speed, poses new challenges and opportunities in the design of advanced control systems.

Nowadays, the demand for accurate position tracking is increasingly evident in a variety of fields, from machine-tool systems to the railway industry and robotic systems (Trojaola et al., 2021; Rao et al., 2022; Guo et al., 2023).

Furthermore, it is well-known that perfect speed tracking would theoretically lead to perfect position tracking. However, the inherent imperfection of dynamic systems prevents achieving this ideal scenario. Therefore, adding a position control loop becomes necessary to address and correct the cumulative errors resulting from poor speed tracking. This integration of a position loop constitutes the basis for a cascade control scheme (Ghidini et al., 2018; Petronijević et al., 2021), allowing for improved overall system performance.

In this context, saturation is a phenomenon that requires special attention in this kind of control scheme (Haidekker, 2020), as it can significantly affect system performance and the ability to meet position objectives. This is why it is common to limit the control signal to the physical limits of the employed actuator. Additionally, the challenges associated with saturation become particularly pronounced when coordinating control actions between interconnected loops, leading to undesired effects such as windup.

The windup effect in cascade control systems typically occurs when the inner loop becomes saturated. In other words, when the inner loop reaches its saturation limits (e.g. the actuator or the physical limitations of the controlled variable), the controller in the inner loop is unable to correct the error, leading to a phenomenon known as windup (Hippe, 2006). It happens because the integral action in the controller continues to integrate the error even when the controller is at its saturation limit. This integrated error accumulates and persists, affecting the performance of the outer loop.

Extensive research has been conducted to develop effective mitigation strategies in addressing the challenges posed by saturation and windup in cascade control systems.

⋆ The authors of this article acknowledge the support of IKERLAN Research Technology Centre (BRTA) and the Computational Intelligence group of UPV/EHU, accredited by the Basque Government (IT1689-22).

Literature has proposed various anti-windup techniques to prevent integrator windup in the presence of saturation (Kumar and Negi, 2012; da Silva et al., 2018; Chen et al., 2023). Commonly employed methods include back-calculation (Fertik and Ross, 1967), integrator clamping (IEEE, 2016), and conditional integration, among others. However, coordinating anti-windup actions between interconnected loops is crucial for optimal performance in the specific context of cascade control systems.

Therefore, this work focuses on addressing the challenges associated with saturation in position control systems by proposing a novel strategy based on saturation synchronisation between control loops. It should be noted that the traction system used is employed to drive a train. Therefore, the simulations are based on controlling the motors that power it to achieve the desired position in the required operating time, complying with the restrictions imposed by the railway network's supervision centre. In this way, this work contributes to the advancement of position control systems in challenging environments, where saturation synchronisation emerges as a pivotal solution to optimise performance and ensure the stability of traction systems. Furthermore, through detailed simulations and practical results, the effectiveness of this strategy in improving the performance of traction systems is demonstrated, especially in windup-prone situations.

The paper is organised as follows. In Section 2, the induction motor model used is briefly described. Section 3 focuses on the development of the cascade position control scheme and how the saturation synchronisation between both control loops is accomplished. The simulations and results are discussed in Section 4, and the conclusions and future works are given in Section 5.

2. INDUCTION MOTOR MODEL

The induction motor model used in this work to validate the proposed motion control is based on the *ikSimscape* library (Rodriguez-Guerra et al., 2019), developed by IKERLAN and built upon the *Simscape* platform. Logically, the model encapsulates the drive responsible for vector control, the inverter, and the induction motor itself.

For the modelling of the induction motor model (Trzynadlowski, 1994), the dynamic equivalent single-phase circuit for a reference frame which rotates at ω_a is used, as shown in figure 1.

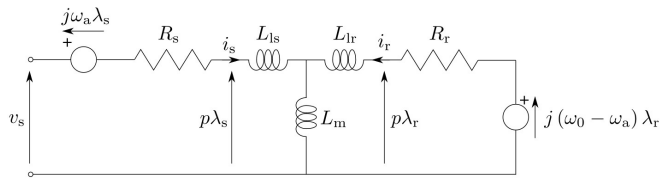

Fig. 1. Dynamic induction motor equivalent single-phase circuit (Trzynadlowski, 1994)

After applying Kirchoff's second law to the motor circuit in figure 1, the electrical behaviour in the dynamic state for a rotating reference frame at angular speed $\omega_e = \omega_a$ can be accurately described as

$$\begin{cases} v_s = R_s i_s + (p + j\omega_e)\lambda_s \\ 0 = R_r i_r + (p + j(\omega_e - \omega_0))\lambda_r \\ \lambda_s = L_s i_s + L_m i_r \\ \lambda_r = L_m i_s + L_r i_r \\ T_e = \dfrac{3}{2} p_p Re(-j\lambda_r i_r^*) \end{cases}, \tag{1}$$

where v_s is the stator voltage space vector, i_s is the stator current space vector, i_r is the referred rotor current space vector, λ_s is the stator flux linkage space vector, λ_r is the rotor flux linkage space vector, ω_0 is the rotor electric rotational speed, ω_e is the reference frame rotational speed, p_p is the number of pairs of poles, $p = \frac{d}{dt}$ is a time derivative operator, T_e is the electric torque produced by the motor, * indicates the complex conjugate, and R_s, R_r, L_s, L_r and L_m are the resistances and inductances that characterised the chosen motor.

The vector control drive and the inverter are necessary to carry out the control over the motor. The vector control drive is based on estimating the rotor and stator flux linkages. This way, the stator voltage needed for the motor to generate the torque associated with the input setpoint can be calculated.

Once the stator voltage reference value is obtained, the inverter transforms direct current i_{dc}, drawn from the DC source, into alternating current i_s. This process enables the calculation of the stator current necessary to power the motor and generate the required torque.

However, for a more in-depth understanding of the vector control drive and the inverter, along with a detailed exposition of the mathematical intricacies governing their roles in the control framework, readers are referred to an upcoming manuscript (Bilbao-Moreno et al., 2024). This manuscript provides a comprehensive analysis of the vector control algorithm, explaining how to estimate rotor and stator flux linkages ($\hat{\lambda}_r$ and $\hat{\lambda}_s$). Furthermore, it also provides a detailed explanation of the inverter's role in transforming direct current (i_{dc}) from the DC source into alternating current (i_s), crucial for precisely modulating the stator voltage to generate the desired output torque. In addition, it delves into other aspects that, although not directly relevant to this current work, are of significant importance for autonomous train control, such as the structure of the automatic train operation system and how the information management between the modules is done.

3. CONTROL SYSTEM ARCHITECTURE

The architecture of the control system employed in this work is based on a cascade position control framework comprising an inner speed loop and an outer position loop. In addition, two feedforward actions are used, based on motor position and obtained after a setpoint planning process (Bilbao et al., 2023). Moreover, considering the motors' maximum traction/braking capability and the speed limit constraints imposed, corresponding saturations have been incorporated into each loop, and the synchronisation between them has been carried out.

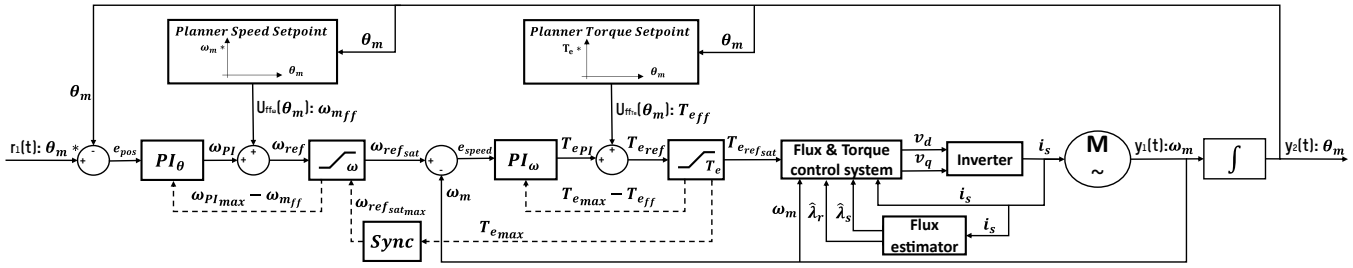

Fig. 2. PI-based cascade position control scheme

As shown by figure 2, the controllers used for both loops have a proportional-integral structure. Logically, the inner loop is first tuned to guarantee zero steady-state error, less than 10% overshoot and a settling time of under 20 seconds. Regarding the outer loop and taking the specifications imposed on the response of the inner loop into account, the internal loop response must be faster than the external loop response. In that way, the outer loop is tuned in order to obtain a settling time greater than 20 seconds, a maximum overshoot of 30% and zero steady-state error.

Considering that the vector control drive and the torque saturation dynamics are faster than the speed loop, they can be neglected in the design. In the same way, the speed saturation dynamic can also be neglected in the design (Alkorta et al., 2016). Thus, the simplified model used to tune both control loops, which are afterwards used to control the detailed model based on *ikSimscape*, is

$$G(s) = \frac{\omega_m(s)}{T_e(s)} = \frac{1}{J\,s}\,, \tag{2}$$

where $G(s)$ represent the transfer function of the simplified model used for the tuning, $\omega_m(s)$ is the output angular speed, $T_e(s)$ is the input torque, J is the total moment of inertia the motor has to overcome, and s is the Laplace operator.

The controllers were tuned using a *robust response time tuning method* (e.g. (Yumuk et al., 2022)) provided by the *Matlab SISOTOOL toolbox*, achieving robust and stable dynamics in closed-loop. Additionally, it should be mentioned that the controllers were designed in discrete time. The values of both controllers after the tuning process are listed in table 1.

Table 1. Parameters of the controllers

Controller	K_p	K_i	T_s
PI_θ	0.42 s^{-1}	0.041 s^{-2}	1 ms
PI_ω	1549.97 $\frac{Nm\,s}{rad}$	194.98 $\frac{Nm}{rad}$	1 ms

Hence, the output for both controllers is defined as

$$\begin{cases} \omega_{PI}(k) = \omega_{ref_{sat}}(k-1) + C_{pos_k}\, e_{pos}(k) + \\ \quad + C_{pos_{k-1}}\, e_{pos}(k-1) - \omega_{m_{ff}}(k-1) \\ T_{e_{PI}}(k) = T_{e_{ref_{sat}}}(k-1) + C_{spd_k}\, e_{spd}(k) + \\ \quad + C_{spd_{k-1}}\, e_{spd}(k-1) - T_{e_{ff}}(k-1) \end{cases}, \tag{3}$$

where

$$\begin{cases} C_{pos_k} = K_{p_\theta} + \dfrac{K_{i_\theta}\,T_s}{2} \\ C_{pos_{k-1}} = \dfrac{K_{i_\theta}\,T_s}{2} - K_{p_\theta} \\ C_{spd_k} = K_{p_\omega} + \dfrac{K_{i_\omega}\,T_s}{2} \\ C_{spd_{k-1}} = \dfrac{K_{i_\omega}\,T_s}{2} - K_{p_\omega} \end{cases}. \tag{4}$$

Here, $\omega_{PI}(k)$ is the output of the controller of the outer loop in the current time instant, $\omega_{ref_{sat}}(k-1)$ is the saturated output of the controller of the outer loop in the previous time instant, $\omega_{m_{ff}}(k-1)$ is the speed feedforward action in the previous time instant, $T_{e_{PI}}(k)$ is the output of the controller of the inner loop in the current time instant, $T_{e_{ref_{sat}}}(k-1)$ is the saturated output of the controller of the inner loop in the previous time instant, $T_{e_{ff}}(k-1)$ is the torque feedforward action in the previous time instant, T_s is the discretisation period, K_{p_ω} and K_{i_ω} are the gains of the inner loop controller and, K_{p_θ} and K_{i_θ} are the gains of the outer loop controller. The remaining parameters are position and speed errors in the current and previous time instants.

Thus, by implementing saturation in both loops, the windup effect is avoided independently in each loop. However, the windup effect persists between both control loops due to the lack of synchronisation between the saturations. Then, in case the inner loop has been saturated at maximum value, in order to find the speed reference of the outer loop associated with this maximum value, it is possible to write the expression associated with $T_{e_{ref_{sat}}}(k)$ as

$$\begin{aligned} T_{e_{max}}(k) = T_{e_{ref_{sat}}}(k-1) + C_{spd_k}\, e_{spd}(k) + \\ + C_{spd_{k-1}}\, e_{spd}(k-1) + T_{e_{ff}}(k) - \,, \\ - T_{e_{ff}}(k-1) \end{aligned} \tag{5}$$

where

$$\begin{cases} e_{spd}(k) = \omega_{ref_{sat}}(k) - \omega_m(k) \\ e_{spd}(k-1) = \omega_{ref_{sat}}(k-1) - \omega_m(k-1) \end{cases} \tag{6}$$

are the speed errors in the current and previous time instants, and $\omega_m(k)$ and $\omega_m(k-1)$ are the motor's output speed in the current and previous time instant.

In this way, it is possible to deduct from equations (5) and (6) the value of $\omega_{ref_{sat_{max}}}(k)$, causing the outer loop to saturate accordingly to the saturation of the inner loop. The expression defining the variable to be synchronised between both loops is

$$\omega_{ref_{sat_{max}}}(k) = \frac{T_{e_{max}}(k) - T_{e_{ref_{sat}}}(k-1)}{C_{spd_k}} - \\ - \frac{C_{spd_{k-1}}\, e_{spd}(k-1) + T_{e_{ff}}(k-1) - T_{e_{ff}}(k)}{C_{spd_k}} + \\ + \omega_m(k) \quad (7)$$

Using (7), when the inner loop saturates, the reference speed value associated with this saturation is calculated, preventing the outer loop from providing a speed setpoint higher than the permissible by the inner loop.

In other words, this value is used in the next iteration of the outer control loop, recalculating $\omega_{ref_{sat}}(k)$ as $\omega_{ref_{sat_{max}}}(k)$, in order not to demand more traction than possible for the traction system.

4. SIMULATION AND RESULTS

As mentioned in the *introduction*, the implemented cascade position control system is focused on its use in railway systems. That is, each motor traction/brakes each of the locomotives that comprise the train.

In other words, this approach guarantees the mitigation of the windup effect between both control loops by calculating the value of the output of the outer controller when the inner controller is saturated at its maximum value.

Therefore, the simulations are based on the assumptions the train must consider, such as speed limits, apparent disturbances on the track, and resistance parameters, which vary depending on the train's speed.

The train modelled is the CHR3 (Xu et al., 2017; Li et al., 2021), which is characterised by table 2.

Table 2. Train parameters

Parameter	Value	Unit
m_1, m_2, m_3, m_4	67.2, 74.6, 74.6, 73	t, t, t, t
C_0	7.75	N/t
C_1	0.228	N s/m t
C_2	0.0166	N s^2/m^2 t
k_1, k_2, k_3	1×10^7	N/m
c_1, c_2, c_3	5×10^6	N s/m

As can be seen in table 2, the train has four cars, which are locomotives and are propelled by the same type of motor. The chosen motor (ABB, 2021) is parametrised as shown in table 3.

Table 3. Parameters of the chosen motor

Parameter	Value	Unit
I_0	188	A
$V_{line-line}$	690	V
I_N	560	A
$cos(\varphi)$	0.85	-
T_N	3524	N m
ω_N	1490	rpm
f_N	50	Hz
$Poles$	4	-
η_N	0.965	-
T_{max}	7400.4	N m
J_{rotor}	8.8	kg m^2

In addition, the motors' tractive and braking capability is characterised as illustrated in figure 3.

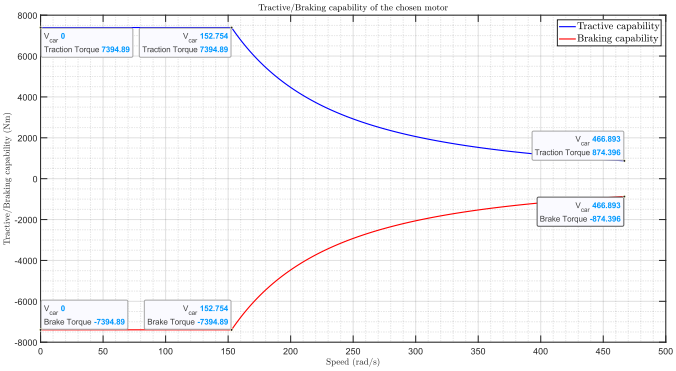

Fig. 3. Electrical tractive/braking capability of the chosen motor

Moreover, the apparent disturbances on the road are presented in table 4.

Table 4. Disturbance parameters on the track

Disturbance	Parameter	Start (rad)	Stop (rad)
Curve	$R_{curve} = 10000$ m	7278.26	9097.82
Slope	$\theta = 1.5$ °	18195.65	36391.3
Tunnel	$L = 200$ m	61865.22	63078.26

In this way, the proposed control system has been simulated with and without synchronisation between the two control loops in order to evaluate its performance. Figure 4 shows the results obtained after running the system with and without applying the synchronised saturation.

The cascade position control scheme used to obtain the results illustrated in figure 4 incorporates position-based feedforward actions to generate speed and torque setpoints. When positioning errors arise, these feedforward actions are adjusted to enable the inner and outer controllers to work together and correct errors, maintaining optimal system performance. In that way, positioning error is reduced during the operation of the train, and the control objective is achieved.

Nevertheless, observable windup effects become apparent without the implementation of synchronised saturation between the two control loops. For instance, during a saturation period of approximately 80 to 110 seconds in the inner loop, the outer loop issues a speed setpoint at the maximum speed limit, even though the inner loop cannot increase its traction setpoint further. In that way, a windup effect can be observed after this period.

In addition, after seconds 155 and 190, another notable example of windup generated due to uncoordinated saturation management between the control loops can be observed. In this instance, when the inner loop saturates, the outer loop also provides a setpoint that exceeds the admissible limit for the inner loop, leading to evident windup effects as depicted in the associated error graph. This uncoordinated response exemplifies the challenge of windup, underscoring the need for an anti-windup mechanism to prevent such scenarios and ensure a more harmonised and effective control strategy.

In this manner, as explained earlier, the saturations between both control loops have been synchronised so that

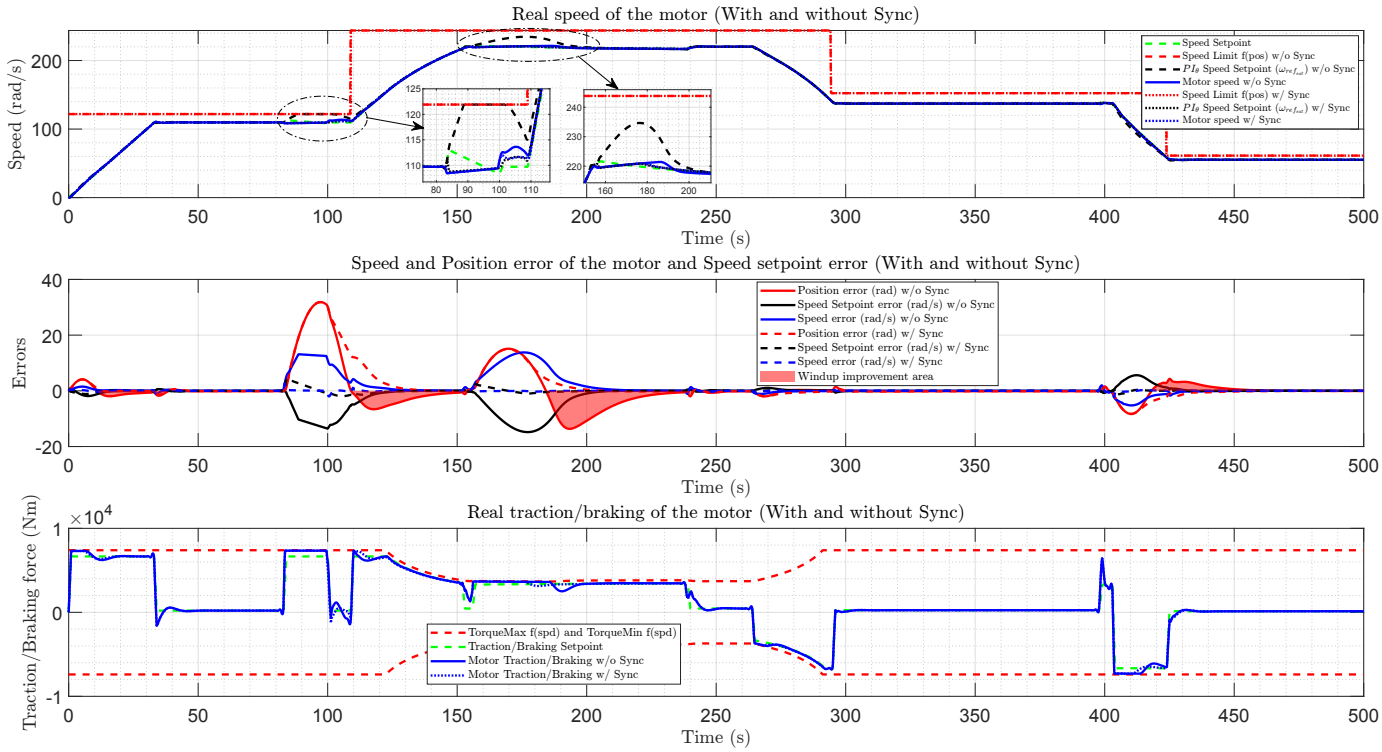

Fig. 4. Response of the cascade position control system for an induction motor with and without saturation synchronisation

when the inner loop is saturated, the outer loop does not provide a higher setpoint.

Analysing the results after implementing the synchronised saturation between both control loops, it is visible how the positioning error is reduced in accordance with the specifications imposed in the outer loop while the windup effects are completely mitigated. Consequently, the train will reach the desired position, and the speed limit imposed is successfully maintained.

The correct implementation of synchronised saturation is evident when comparing both results. During seconds 80 and 110, corresponding to inner loop saturation, the outer loop provides a setpoint that adheres to the admissible limits. Unlike previous results, the outer loop intelligently adjusts, ensuring it does not exceed the maximum speed limit. Another notable example occurs between 155 and 190 seconds, where the speed setpoint provided by the outer loop is deliberately reduced compared with the results without the synchronisation, responding to the saturation in the inner loop.

Additionally, the results associated with positioning error may appear confusing because positive errors when accelerating and negative errors when decelerating while the inner loop is saturated do not vary between both methods. It happens because the inner loop is saturated, and it is not possible to make corrections at this level, requiring a replanning by the previously mentioned setpoint planning process. However, the reduction in positioning error immediately after these instances is noteworthy due to the application of the implemented anti-windup method, as seen in the windup improvement area. Furthermore, after calculating the performance indices (IAE) for each of the cases in the windup improvement area, it is deduced that the controller with the anti-windup strategy has better results (IAE=865.3 rad s) than the controller without this strategy (IAE=1035.5 rad s). This analysis excludes the saturation error zones.

In summary, using torque and speed motor setpoints as feedforward actions based on the motors' current position enables the system to navigate track disturbances adeptly. Simultaneously, the position setpoint serves as the initial reference for the control system, generating the necessary torque to propel and brake the train until it reaches the desired position. In addition, synchronised saturation allows for better results than basic implementation, where the external controller generates overly aggressive control signals.

5. CONCLUSION AND FUTURE WORKS

In this work, the traction control system of a train has been developed. For this purpose, a cascade control architecture, which incorporates feedforward actions, saturation at the output of each controller, and synchronisation between both loops to avoid windup generation, has been used.

From the results, it can be concluded that adding a windup mitigation mechanism significantly improves the system response, reducing the control effort of the designed controllers, as it avoids the generation of overly aggressive speed setpoints by the external controller when the inner loop is already saturated.

In terms of future directions, the main objective will be to simulate the system considering uncertainties in the parameters of the train, such as the masses that refer to each of the cars of the train, which translates into a

variation in the moment of inertia to be overcome by the motors. In addition, delayed or advanced appearances of disturbances on the track will be applied, whereby the setpoints provided for the cascade control scheme used will not be valid. Therefore, the system state variables will be feedback to the setpoint planner, and setpoints will be adapted at runtime.

ACKNOWLEDGEMENTS

This work is part of a doctoral thesis proposed by the department of Mechatronic Technologies of IKERLAN Research Technology Centre, a member of BRTA. In this way, the authors would like to thank the continuous support and collaboration of both IKERLAN and the Computational Intelligence group of the UPV/EHU, accredited by the Basque Government (IT1689-22).

REFERENCES

ABB (2021). High voltage engineered induction motors - technical catalog. URL.

Alkorta, P., Barambones, O., Vicandi, F.J., Cortajarena, J.A., and Martija, I. (2016). Effective proportional derivative position control of induction motor drives. In *2016 IEEE International Conference on Industrial Technology (ICIT)*, 147–152. doi:10.1109/ICIT.2016.7474741.

Bilbao, D., Elorza, I., and Irigoyen, E. (2023). Development and simulation of the automatic train operation subsystem. In *XLIV Jornadas de Automática*, 132–137. doi:10.17979/spudc.9788497498609.132.

Bilbao-Moreno, D., Elorza, I., and Irigoyen, E. (2024). Development of a software platform for automatic train operation: Integrating meso- and microscopic layers. Manuscript in preparation.

Chen, J., Ge, C., Qiang, D., Geng, H., O'Donnell, T., and Milano, F. (2023). Impact of frequency anti-windup limiter on synchronization stability of grid feeding converter. *CSEE Journal of Power and Energy Systems*, 9(5), 1676–1687. doi:10.17775/CSEEJPES.2022.06230.

da Silva, L.R., Flesch, R.C., and Normey-Rico, J.E. (2018). Analysis of anti-windup techniques in pid control of processes with measurement noise. *IFAC-PapersOnLine*, 51(4), 948–953. doi:10.1016/j.ifacol.2018.06.100. 3rd IFAC Conference on Advances in Proportional-Integral-Derivative Control PID 2018.

Dantas, A., Dantas, A., Campos, J., Neto, D., and Dorea, C. (2018). Pid control for electric vehicles subject to control and speed signal constraints. *Journal of Control Science and Engineering*, 2018, 1–11. doi:10.1155/2018/6259049.

Fertik, H.A. and Ross, C.W. (1967). Direct digital control algorithm with anti-windup feature. *ISA transactions*, 6(4), 317.

Ghidini, S., Beschi, M., Pedrocchi, N., and Visioli, A. (2018). Robust tuning rules for series elastic actuator pid cascade controllers. In *3rd IFAC Conference on Advances in Proportional-Integral-Derivative Control PID 2018*, volume 51, 220–225. doi:10.1016/j.ifacol.2018.06.069.

Guo, Y., Sun, P., Feng, X., and Yan, K. (2023). Adaptive fuzzy sliding mode control for high-speed train using multi-body dynamics model. *IET Intelligent Transport Systems*, 17(2), 450 – 461. doi:10.1049/itr2.12270.

Haidekker, M.A. (2020). 9 - linearization of nonlinear components. In M.A. Haidekker (ed.), *Linear Feedback Controls (Second Edition)*, 133–143. Elsevier. doi:10.1016/B978-0-12-818778-4.00017-0.

Hippe, P. (2006). *Windup in Control: Its Effects and Their Prevention*. Springer. doi:10.1007/1-84628-323-X.

IEEE (2016). Ieee recommended practice for excitation system models for power system stability studies. *IEEE Std 421.5-2016 (Revision of IEEE Std 421.5-2005)*, 1–207. doi:10.1109/IEEESTD.2016.7553421.

Kumar, S. and Negi, R. (2012). A comparative study of pid tuning methods using anti-windup controller. In *2012 2nd International Conference on Power, Control and Embedded Systems*, 1–4. doi:10.1109/ICPCES.2012.6508138.

Li, Z., Ni, C., and Huang, D. (2021). Robust h_∞ cruise control of high-speed train with parameter uncertainties, time-varying delays and disturbance. In *2021 IEEE 16th Conference on Industrial Electronics and Applications (ICIEA)*, 1901–1906. doi:10.1109/ICIEA51954.2021.9516046.

Maxwell, J.C. (1868). On governors. *Proceedings of the Royal Society of London*, 16, 270–283. doi:10.1098/rspl.1867.0055.

Petronijević, M.P., Čedomir Milosavljević, Veselić, B., Peruničić-Draženović, B., and Huseinbegović, S. (2021). Robust cascade control of electrical drives using discrete-time chattering-free sliding mode controllers with output saturation. *Electrical Engineering*, 103, 2181–2195. doi:10.1007/s00202-020-01198-x.

Rao, J., Li, B., Zhang, Z., Chen, D., and Giernacki, W. (2022). Position control of quadrotor uav based on cascade fuzzy neural network. *Energies*, 15(5). doi:10.3390/en15051763.

Rodriguez-Guerra, J., Calleja, C., Elorza, I., Macarulla, A.M., Pujana, A., and Azurmendi, I. (2019). A methodology for real-time hil validation of hydraulic-press controllers based on novel modeling techniques. *IEEE Access*, 7, 110541–110553. doi:10.1109/ACCESS.2019.2934170.

Shakouri, P., Ordys, A., Laila, D., and Askari, M. (2011). Adaptive cruise control system: Comparing gain-scheduling pi and lq controllers. *IFAC Proceedings Volumes*, 44(1), 12964–12969. doi:10.3182/20110828-6-IT-1002.02250. 18th IFAC World Congress.

Trojaola, I., Elorza, I., Irigoyen, E., Pujana-Arrese, A., and Sorrosal, G. (2021). An innovative mimo iterative learning control approach for the position control of a hydraulic press. *IEEE Access*, 9, 146850 – 146867. doi:10.1109/ACCESS.2021.3123668.

Trzynadlowski, A.M. (1994). *The Field Orientation Principle in Control of Induction Motors*. Springer US. doi:10.1007/978-1-4615-2730-5.

Xu, Z., Huang, Z., Gao, K., Li, S., Zhang, R., and Liu, W. (2017). Optimal operation of high-speed train using hybrid model predictive control. In *2017 29th Chinese Control And Decision Conference (CCDC)*, 3642–3647. doi:10.1109/CCDC.2017.7979137.

Yumuk, E., Copot, C., and Ionescu, C.M. (2022). A robust auto-tuning pid controller design based on s-shaped time domain response. In *8th International Conference on Control, Decision and Information Technologies*, 525–530. doi:10.1109/CoDIT55151.2022.9804065.